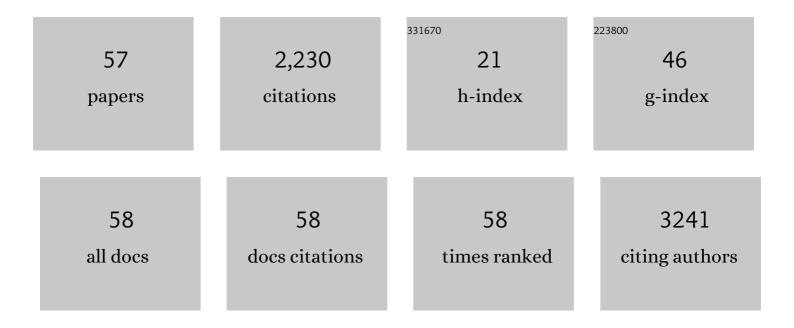
## Jiwen Feng

List of Publications by Year in descending order

Source: https://exaly.com/author-pdf/7033194/publications.pdf Version: 2024-02-01



INVEN FENC

#	Article	IF	CITATIONS
1	Manipulating Adsorption–Insertion Mechanisms in Nanostructured Carbon Materials for Highâ€Efficiency Sodium Ion Storage. Advanced Energy Materials, 2017, 7, 1700403.	19.5	662
2	Mobile Ions in Composite Solids. Chemical Reviews, 2020, 120, 4169-4221.	47.7	193
3	An Overall Understanding of Sodium Storage Behaviors in Hard Carbons by an "Adsorptionâ€Intercalation/Filling―Hybrid Mechanism. Advanced Energy Materials, 2022, 12, .	19.5	121
4	Hydrophobic modification of cellulose nanocrystal via covalently grafting of castor oil. Cellulose, 2013, 20, 179-190.	4.9	112
5	Rotational Cluster Anion Enabling Superionic Conductivity in Sodium-Rich Antiperovskite Na <sub>3</sub> OBH <sub>4</sub> . Journal of the American Chemical Society, 2019, 141, 5640-5644.	13.7	97
6	Methylsulfonylmethane-Based Deep Eutectic Solvent as a New Type of Green Electrolyte for a High-Energy-Density Aqueous Lithium-Ion Battery. ACS Energy Letters, 2019, 4, 1419-1426.	17.4	87
7	In-Channel and In-Plane Li Ion Diffusions in the Superionic Conductor Li <sub>10</sub> GeP <sub>2</sub> S <sub>12</sub> Probed by Solid-State NMR. Chemistry of Materials, 2015, 27, 5503-5510.	6.7	75
8	lon-selective copper hexacyanoferrate with an open-framework structure enables high-voltage aqueous mixed-ion batteries. Journal of Materials Chemistry A, 2017, 5, 16740-16747.	10.3	74
9	Effect of Urea on Phase Transition of Poly( <i>N</i> -isopropylacrylamide) and Poly( <i>N</i> , <i>N</i> -diethylacrylamide) Hydrogels: A Clue for Urea-Induced Denaturation. Macromolecules, 2016, 49, 234-243.	4.8	63
10	<sup>1</sup> H MAS NMR Studies of the Phase Separation of Poly( <i>N</i> -isopropylacrylamide) Gel in Binary Solvents. Langmuir, 2009, 25, 5898-5902.	3.5	50
11	Polyethylene Glycol–Na <sup>+</sup> Interface of Vanadium Hexacyanoferrate Cathode for Highly Stable Rechargeable Aqueous Sodium-Ion Battery. ACS Applied Materials & Interfaces, 2019, 11, 28762-28768.	8.0	41
12	<sup>1</sup> H HRMAS NMR Study on Phase Transition of Poly( <i>N</i> -isopropylacrylamide) Gels with and without Grafted Comb-Type Chains. Macromolecules, 2009, 42, 2074-2078.	4.8	36
13	Dimensionality-dependent photocatalytic activity of TiO2-based nanostructures: nanosheets with a superior catalytic property. Journal of Materials Science, 2013, 48, 5171-5179.	3.7	34
14	Novel Sodium–Poly(tartaric acid)Borate-Based Single-Ion Conducting Polymer Electrolyte for Sodium–Metal Batteries. ACS Applied Energy Materials, 2020, 3, 10053-10060.	5.1	34
15	Phase Transition and Preferential Alcohol Adsorption of Poly( <i>N</i> , <i>N</i> -diethylacrylamide) Gel in Water/Alcohol Mixtures. Macromolecules, 2015, 48, 1126-1133.	4.8	29
16	Solid-state NMR characterizations on phase structures and molecular dynamics of poly(ethylene-co-vinyl acetate). Journal of Polymer Science, Part B: Polymer Physics, 2006, 44, 2864-2879.	2.1	27
17	Microstructure and thermal properties of ethylene-(vinyl acetate) copolymer/rectorite nanocomposites. Polymer International, 2006, 55, 312-318.	3.1	25
18	Novel hierarchical porous carbon prepared by a one-step template route for electric double layer capacitors and Li–Se battery devices. Journal of Materials Chemistry A, 2020, 8, 4376-4385.	10.3	25

JIWEN FENG

#	Article	IF	CITATIONS
19	Preferential adsorption of the additive is not a prerequisite for cononsolvency in water-rich mixtures. Physical Chemistry Chemical Physics, 2017, 19, 30097-30106.	2.8	24
20	Dissolution of chitin in aqueous KOH. Cellulose, 2016, 23, 1705-1711.	4.9	23
21	Inverse solubility of chitin/chitosan in aqueous alkali solvents at low temperature. Carbohydrate Polymers, 2019, 206, 487-492.	10.2	22
22	Li–Se batteries: Insights to the confined structure of selenium in hierarchical porous carbon and discharge mechanism in the carbonate electrolyte. Carbon, 2022, 191, 122-131.	10.3	22
23	Ultralow field NMR spectrometer with an atomic magnetometer near room temperature. Journal of Magnetic Resonance, 2013, 237, 158-163.	2.1	21
24	Bimetallic NiCoP nanoparticles incorporating with carbon nanotubes as efficient and durable electrode materials for dye sensitized solar cells. Journal of Alloys and Compounds, 2019, 788, 198-205.	5.5	21
25	Nitrogen and sulfur dual-doped chitin-derived carbon/graphene composites as effective metal-free electrocatalysts for dye sensitized solar cells. Applied Surface Science, 2018, 441, 807-815.	6.1	20
26	High stable rate cycling performances of microporous carbon spheres/selenium composite (MPCS/Se) cathode as lithium–selenium battery. Journal of Power Sources, 2020, 473, 228611.	7.8	19
27	Effect of surface acetylatedâ€chitin nanocrystals on structure and mechanical properties of poly(lactic acid). Journal of Applied Polymer Science, 2014, 131, .	2.6	18
28	Low concentration electrolyte with non-solvating cosolvent enabling high-voltage lithium metal batteries. IScience, 2022, 25, 103490.	4.1	17
29	Efficient organic dyes based on perpendicular 6,12-diphenyl substituted indolo[3,2-b]carbazole donor. Photochemical and Photobiological Sciences, 2016, 15, 1514-1523.	2.9	16
30	Effects of end groups on phase transition and segmental mobility of poly( <i>N</i> â€isopropylacrylamide) chains in D <sub>2</sub> O. Journal of Polymer Science, Part B: Polymer Physics, 2011, 49, 749-755.	2.1	15
31	Effect of Halogen Doping in Sodium Solid Electrolytes Based on the Na–Sn–Si–P–S Quinary System. Chemistry of Materials, 2020, 32, 4065-4071.	6.7	15
32	36â€Nuclearity Organophosphonateâ€Functionalized Polyoxomolybdates: Synthesis, Characterization and Selective Catalytic Oxidation of Sulfides. Chemistry - A European Journal, 2020, 26, 14896-14902.	3.3	14
33	Effects of electron irradiation on poly(vinylidene fluoride–trifluoroethylene) copolymers studied by solid-state nuclear magnetic resonance spectroscopy. Journal of Polymer Science, Part B: Polymer Physics, 2006, 44, 1714-1724.	2.1	12
34	Crystalline Phases in Ethylene Copolymers Studied by Solid-State NMR and DSC. Macromolecules, 2010, 43, 5713-5722.	4.8	12
35	Quantitative NMR investigation on the low-temperature dissolution mechanism of chitin in NaOH/urea aqueous solution. Cellulose, 2015, 22, 2221-2229.	4.9	11
36	Highly mobile segments in crystalline poly(ethylene oxide)8:NaPF6 electrolytes studied by solid-state NMR spectroscopy. Journal of Chemical Physics, 2014, 140, 074901.	3.0	10

Jiwen Feng

#	Article	IF	CITATIONS
37	A poly(1,3-dioxolane) based deep-eutectic polymer electrolyte for high performance ambient polymer lithium battery. Materials Today Physics, 2022, 22, 100620.	6.0	10
38	Anomalous diffusion of chains in semicrystalline ethylene polymers. Journal of Chemical Physics, 2009, 130, 184709.	3.0	9
39	Efficient ï€-conjugated interrupted host polymer by metal-free polymerization for blue/green phosphorescent light-emitting diodes. Journal of Polymer Science Part A, 2014, 52, 1037-1046.	2.3	9
40	Synergy of Singleâ€ion Conductive and Thermoâ€responsive Copolymer Hydrogels Achieving Antiâ€Arrhenius Ionic Conductivity. Chemistry - an Asian Journal, 2019, 14, 1404-1408.	3.3	9
41	New Li <sub>10</sub> GeP <sub>2</sub> S <sub>12</sub> Structure Ordering and Li-Ion Dynamics Unveiled in Li <sub>4</sub> GeS <sub>4</sub> –Li <sub>3</sub> PS <sub>4</sub> Superionic Conductors: A Solid-State Nuclear Magnetic Resonance Study. ACS Applied Materials & amp; Interfaces, 2020, 12, 27029-27036.	8.0	9
42	In Situ Characterization of Over-Lithiation of Organosulfide-Based Lithium Metal Anodes. ACS Applied Materials & Interfaces, 2021, 13, 41555-41562.	8.0	9
43	Bipolar π-conjugation interrupted host polymers by metal-free superacid-catalyzed polymerization for single-layer electrophosphorescent diodes. RSC Advances, 2014, 4, 50027-50034.	3.6	8
44	Decorating titanate nanotubes with protonated 1,2,4-triazole moieties for anhydrous proton conduction. Journal of Colloid and Interface Science, 2014, 432, 26-30.	9.4	8
45	Dynamic mechanism of halide salts on the phase transition of protein models, poly(N-isopropylacrylamide) and poly(N,N-diethylacrylamide). Physical Chemistry Chemical Physics, 2020, 22, 12644-12650.	2.8	8
46	Preparation and characterization of curdlan with unique single-helical conformation and its assembly with Congo Red. Carbohydrate Polymers, 2021, 263, 117985.	10.2	8
47	A peripheral component interconnect express-based scalable and highly integrated pulsed spectrometer for solution state dynamic nuclear polarization. Review of Scientific Instruments, 2015, 86, 083101.	1.3	7
48	Hybrid films of PEDOT containing transition metal phosphates as high effective Pt-free counter electrodes for dye sensitized solar cells. Organic Electronics, 2018, 57, 171-177.	2.6	7
49	Characterizing oils in oil-water mixtures inside porous media by Overhauser dynamic nuclear polarization. Fuel, 2019, 257, 116107.	6.4	6
50	Simultaneous acquisition of multi-nuclei enhanced NMR/MRI by solution-state dynamic nuclear polarization. Science China Chemistry, 2016, 59, 830-835.	8.2	4
51	LiFePO4/TiO2/Pt composite film used as effective and robust counter electrode for dye sensitized solar cells. Journal of Materials Science: Materials in Electronics, 2017, 28, 18396-18403.	2.2	4
52	Inhomogeneous-collapse driven micelle–vesicle transition of amphiphilic block copolymers. Soft Matter, 2017, 13, 7106-7111.	2.7	4
53	Selective Blockage of Li-Ion Diffusion Pathways in Li <sub>10</sub> SnP <sub>2</sub> S <sub>12</sub> : Insights from Nuclear Magnetic Resonance. Journal of Physical Chemistry C, 2021, 125, 27884-27890.	3.1	4
54	Gradient shimming based on regularized estimation for B0-field and shim functions. Journal of Magnetic Resonance, 2016, 268, 1-9.	2.1	3

#	Article	IF	CITATIONS
55	Dynamics and Glass Transition of Supercooled Water Confined in Amphiphilic Polymer Films. Journal of Physical Chemistry Letters, 2020, 11, 6039-6044.	4.6	2
56	THz-enhanced dynamic nuclear polarized liquid spectrometer. Journal of Magnetic Resonance, 2021, 330, 107044.	2.1	1
57	A Digital Distributed Spectrometer for Dual-nuclei Simultaneous MRI. , 2021, , .		1